Protein–Inhibitor Complexes

DOI: 10.1002/anie.200802915

The Absolute Configuration of Rhizopodin and Its Inhibition of Actin Polymerization by Dimerization**

*Gregor Hagelueken, Simone C. Albrecht, Heinrich Steinmetz, Rolf Jansen, Dirk W. Heinz, Markus Kalesse, and Wolf-Dieter Schubert**

In 1993 the novel polyketide rhizopodin (Figure 1) was isolated from the myxobacterium *Myxococcus stipitatus*.[1] Rhizopodin was found to dramatically affect the cytoskeleton of eukaryotic cells even at nanomolar concentrations,[2] an ability traced to its property of binding and thereby inhibiting the polymerization of actin. The structure of rhizopodin was proposed to consist of a 16-membered macrolide ring bearing nine stereogenic centers, a disubstituted oxazole ring, and a conjugated diene system (Figure 1a).

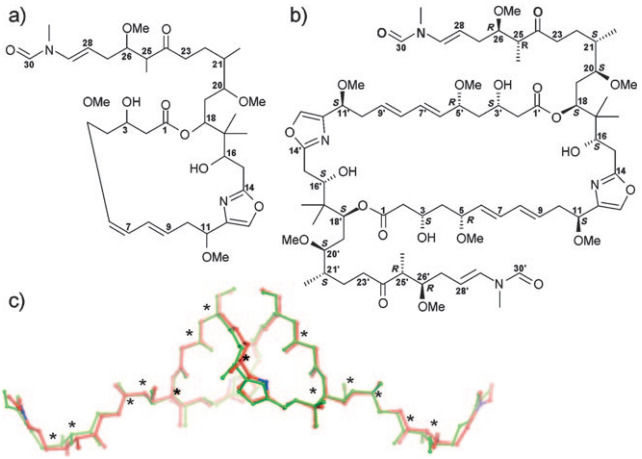

Figure 1. Structure of rhizopodin. a) Originally proposed monolactone structure. b) Revised, C_2-symmetric dilactone structure including stereochemistry. c) Ball-and-stick model of the biologically active conformation of rhizopodin. The C_2 symmetry is demonstrated by the superposition of rhizopodin (green) with a copy rotated by 180° (red). The stereochemical assignment of stereogenic centers related by C_2 symmetry (asterisks) is consistent.

To investigate the binding mode of rhizopodin to G-actin and to establish its absolute configuration, we elucidated the structure of rhizopodin in its complex with rabbit muscle G-actin by X-ray crystallography. Solving the crystal structure at 2.4 Å resolution, we unexpectedly identified a C_2-symmetric, 38-membered dilactone exhibiting 18 chiral centers, two disubstituted oxazole rings, and two conjugated diene systems. Based on the crystal structure, we describe herein the biologically active conformation of this rhizopodin dilactone and the absolute configuration of the 18 stereogenic centers.

Pyrene-labeled G-actin was used to analyze the interaction of rhizopodin with purified G-actin by in vitro polymerization assays. Increasing amounts of rhizopodin serve to increasingly inhibit actin polymerization. A rhizopodin dilactone/actin stoichiometry of 1:2 suffices to completely inhibit actin polymerization. The elution volume of rhizopodin-complexed G-actin in gel-filtration chromatography is correspondingly reduced, implying rhizopodin-mediated dimerization of G-actin. In vivo, incorporation of rhizopodin-poisoned actin molecules into growing actin filaments would cap the latter, such that significantly lower rhizopodin/actin stoichiometries would suffice to severely disrupt the actin cytoskeleton dynamics.

We solved the crystal structure of orthorhombic rhizopodin/actin crystals at a resolution of 2.4 Å by molecular replacement using the structure of tetramethylrhodamine (TMR)-labeled rabbit actin (PDB: 1J6Z) as a search model.[3,4] Two actin molecules (monomers A and B) occupy the asymmetric unit; they are related by a non-crystallographic, twofold rotational symmetry axis perpendicular to the crystallographic *c* axis. Crystallographic data and refinement statistics are listed in Table 1.

The conformations of the actin monomers A and B are largely identical (root mean square deviation = 0.5 Å, Figure 2a) and similar to other structures of G-actin. Each monomer binds one molecule of ATP between subdomains 2 and 4.[5,6] Monomer A is overall well-defined except for a disordered DNAse-binding-loop of subdomain 2 (residues 40–53). In monomer B, subdomain 2 (32–70) and a loop of subdomain 4 (residues 199–204) are disordered and hence not evident in the electron density map.

A first electron density map of the partially refined structure[7] revealed residual electron density in the cleft between subdomains 1 and 3 (Figure 2b). This region of actin also serves as a binding site for polymerization-inhibiting

[*] G. Hagelueken, S. C. Albrecht, Dr. W.-D. Schubert
Research Group Molecular Host–Pathogen Interactions
Helmholtz-Centre for Infection Research
Inhoffenstrasse 7, 38124 Braunschweig (Germany)
Fax: (+49) 531-6181-7099
E-mail: wolf-dieter.schubert@helmholtz-hzi.de
Prof. D. W. Heinz
Division of Structural Biology
Helmholtz-Centre for Infection Research, Braunschweig (Germany)
Dipl.-Chem. H. Steinmetz, Dr. R. Jansen, Prof. M. Kalesse
Departments of Microbial Drugs and Medicinal Chemistry
Helmholtz-Centre for Infection Research, Braunschweig (Germany)

[**] This work was supported by the Deutsche Forschungsgemeinschaft as part of the Priority Program 1150 (SCHU 1560/1-1 to 1-3). Beam time and support by X12 beamline staff (EMBL Hamburg outstation, DESY) is gratefully acknowledged. Coordinates of the actin/rhizopodin complex have been deposited in the Protein Data Bank under access number 2VYP.

Supporting information for this article is available on the WWW under http://dx.doi.org/10.1002/anie.200802915.

Table 1: Crystallographic data.

Diffraction data	
space group	$P2_12_12$
cell dimensions [Å]	77.7 (*a*), 194.9 (*b*), 53.0 (*c*)
resolution [Å]	97.6–2.3 (2.5–2.3)[a]
$I/\sigma(I)$	28.4 (3.5)[a]
completeness [%]	99.8 (99.5)[a]
redundancy	8.0 (7.4)[a]
R_{merge} [%]	4.7 (55.0)[a]
Wilson B [Å^2]	45.0
Refinement:	
resolution [Å]	97.6–2.35 (2.41-2.35)[a]
R_{work} [%]	19.0
R_{free} [%]	24.4
atoms (protein/ligand/water)	5483/104/212
B factors (Å^2; protein/ligand/water)	42/30/41
rmsd bonds [Å]/angles [°]	0.017/1.7
Ramachandran favored/outliers [%]	97.2/0.3

[a] Data in parentheses represent the shell of highest resolution.

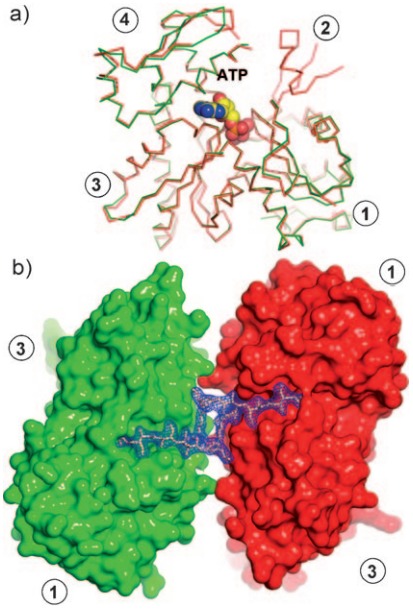

Figure 2. Structure of the G-actin monomers A (red) and B (green). a) Superposition of the crystallographically independent monomers. Numbers denote the four subdomains of G-actin. ATP, bound in the cleft between subdomains 2 and 4, is shown as a CPK model (C yellow, N blue, O red, P orange). b) The asymmetric unit of the actin/rhizopodin crystal contains monomer A (red) and monomer B (green), which are shown as molecular surfaces. The blue mesh represents a rhizopodin omit map (F_o-F_c, 2σ) following model perturbation and re-refinement. Rhizopodin is seen to bind in the cleft between subdomains 1 and 3.

proteins such as gelsolin,[8] small molecules such as TMR,[3] and other macrolide polymerization inhibitors.[5,6,9] As we assumed rhizopodin to be a monomeric lactone as previously reported, we modeled the difference electron density as two monomeric rhizopodin molecules. Owing to the relative orientation of the G-actin monomers A and B, the macrolide rings of the two rhizopodin monomers are placed directly opposite each other with their diene moieties in close proximity (Figure 3a). The enamide side chains and the adjoining regions of the macrolide ring perfectly match the observed electron density, resulting in optimal refinement.

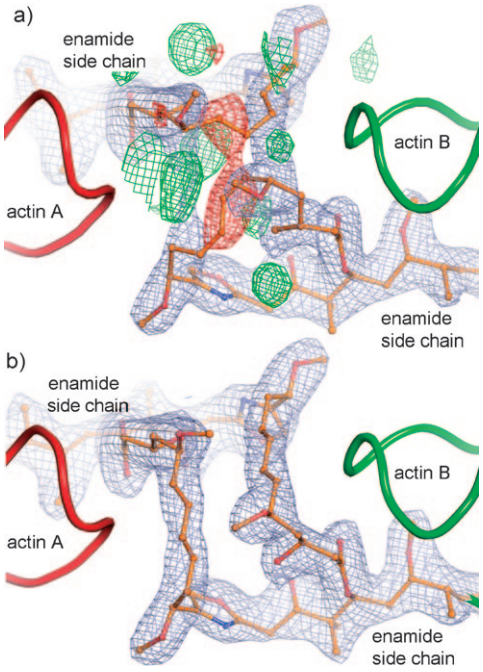

Figure 3. Three-dimensional representation of the rhizopodin/actin complex. a) The monomeric rhizopodin macrolide (ball-and-stick model; N blue, C orange, O red) does not provide an optimal explanation of the electron density (blue mesh: $2F_o-F_c$, 1σ) and results in significant difference density (F_o-F_c, green, 3σ; red, -3σ). Parts of the actin monomers are shown as a cartoon model and colored as in Figure 2. b) The revised model of rhizopodin (Figure 1) provides an optimal fit to the electron density.

However, the region of the two macrolide rings opposite the enamide side chain could not be accommodated satisfactorily, which resulted in significant difference density (Figure 3a). Careful inspection of the electron density map indicated that a homodimeric rhizopodin dilactone would provide a better model. The inferred dimeric structure could be suitably refined (Figure 3b), and it immediately explains the observed dimerization of G-actin described above: A C_2-symmetric rhizopodin dilactone bears two enamide side chains, each of which binds a single G-actin molecule, resulting in a ternary rhizopodin/G-actin complex. Analysis of rhizopodin by mass spectrometry correspondingly reveals a mass peak at 1470 Da (see the Supporting Information). Evidence for a monolactone could, by contrast, not be inferred, while higher oligomers can be ruled out. (For detailed analysis of ^{13}C NMR spectra and MS data, see the Supporting Information.) Our suggestion of a C_2-symmetric rhizopidin dilactone in some ways mirrors the case of the antibiotic vermiculine, which was also found to be a C_2-symmetric molecule rather than monomeric, as originally proposed.[10]

Qualitatively the rhizopodin difference electron density was such that the chirality of all 18 stereogenic centers could be identified. The chirality was not restrained during refine-

ment. As a consequence of the non-crystallographic C_2 symmetry of the observed rhizopodin dilactone, these assignments could be internally corroborated. Pairs of stereogenic centers were invariably found to be equivalent.

Rhizopodin, and in particular its enamide side chain, is remarkably well adapted to the molecular surface of actin (Figure 4). Recognition is primarily achieved through van der

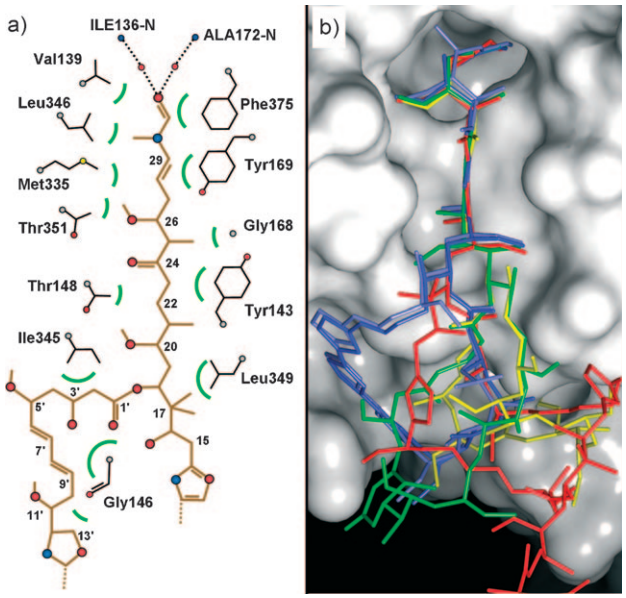

Figure 4. Binding of rhizopodin to G-actin. a) Schematic representation of rhizopodin (C orange, N blue, O red) recognition by hydrophobic residues of G-actin (black). Van der Waals interactions are shown as green arcs, water molecules as red spheres, and hydrogen bonds as dotted lines. b) Superposition of related inhibitors bound to actin (white surface). Red: rhizopodin, green: sphinxolide B, yellow: reidispongiolide A, lilac: kabiramide C, blue: jaspisamide A.

Waals interactions of the enamide side chain with the hydrophobic residues in the binding cleft of actin. The only polar interactions involve two water-mediated hydrogen bonds of the terminal carbonyl oxygen of rhizopodin to the backbone nitrogen atoms of Ile136 and Ala172. The conformation of the enamide side chain is similar to that of other macrolides such as kabiramide, reidisphingolid,[2,6] and sphinxolid.[5] The complex of G-actin with bistramide A, a macrolide with a structurally divergent side chain, indicates that physically blocking the 1–3 cleft suffices to prevent actin polymerization.[11] This inference is reinforced by the fact that the macrolide rings of the other inhibitors are structurally distinct, each interacting with a different set of residues on the molecular surface of actin (Figure 4b).

The crystal structure of the functional complex between actin and rhizopodin unexpectedly reveals a C_2-symmetric rhizopodin dilactone. The well-defined difference electron density allows us to assign the absolute configuration of each of the 18 stereogenic centers. Because of the C_2 symmetry, the stereochemistry may be internally corroborated, ensuring an accurate absolute definition of configuration (Figure 1c). This structure illustrates how a small symmetric molecule can bring about a bulky actin complex (Figure 2b), which would create a significant obstacle to actin polymerization in eukaryotic cells and thereby explains the dramatic effect of rhizopodin in vivo.[2]

Experimental Section

Actin was purified from rabbit muscle acetone powder[11] and stored in G-buffer (2 mM Hepes pH 7.5, 0.2 mM ATP, 1 mM β-mercaptoethanol, 0.2 mM $CaCl_2$). The protein was purified by ceramic hydroxyapatite (BIO-RAD) chromatography using G-buffer without ATP as the elution buffer (buffer A). Cationic impurities were eluted using a linear gradient from buffer A to buffer B (buffer A + 500 mM KCl). The acidic actin eluted in a second gradient from buffer A to buffer C (buffer A + 500 mM KH_2PO_4/K_3PO_4).

N-(1-pyrene)-iodoacetamide-labeled actin (pyrene-actin) was used for polymerization assays.[13] A typical experiment (1 mL) contained 11 μM G-actin and 1 μM pyrene-actin in G-buffer. Polymerization was induced by adding 100 μL 20 mM Hepes pH 7.5, 500 mM KCl, 10 mM $MgCl_2$. Rhizopodin was added in concentrations between 2.2 to 22 μM. Pyrene fluorescence was excited at 365 nm and recorded at 385 nm using a Perkin–Elmer LS50B spectrometer.

The actin/rhizopodin complex (ratio of 1:2) was purified by gel-filtration chromatography using a Superdex 200 10/30 column (GE-Healthcare) and G-Buffer with 25 mM KCl as elution buffer. After elution the complex was immediately dialyzed against G-buffer.

Crystals of the purified actin/rhizopodin complex were grown by hanging-drop vapor diffusion at a temperature of 20°C. A 3 μL portion of the actin/rhizopodin complex was mixed with 3 μL of a reservoir solution containing 100 mM MES pH 6.6, 14% (w/v) PEG1500, 12% (w/v) 1,6-hexanediol, 100 mM $CaCl_2$, 1 mM DTT, 10 mM betaine hydrochloride. The size of crystals was improved by microseeding techniques. Cryoprotection was achieved by transferring crystals to a reservoir solution supplemented with 15% PEG400 immediately prior to flash-cooling in liquid nitrogen.

Diffraction data were collected at a wavelength of 1.07 Å on a 225 mm Marmosaic CCD detector (beamline X12, EMBL, DESY, Hamburg, Germany). The data were processed with HKL2000.[14] The structure was solved by molecular replacement using Phaser,[4] refined with Refmac,[7] and manually optimized using Coot.[15] The Monomer Library Sketcher[16] was used to build the rhizopodin models. Figures were prepared with Pymol (www.pymol.org).

Received: June 18, 2008
Revised: October 3, 2008
Published online: November 26, 2008

Keywords: actin · inhibitors · macrolides · myxobacteria · rhizopodin

[1] F. Sasse, H. Steinmetz, G. Höfle, H. Reichenbach, *J. Antibiot.* **1993**, *46*, 741–748.
[2] T. M. Gronewold, F. Sasse, H. Lünsdorf, H. Reichenbach, *Cell Tissue Res.* **1999**, *295*, 121–129.
[3] L. R. Otterbein, P. Graceffa, R. Dominguez, *Science* **2001**, *293*, 708–711.
[4] A. J. McCoy, R. W. Grosse-Kunstleve, L. C. Storoni, R. J. Read, *Acta Crystallogr. Sect. D* **2005**, *61*, 458–464.
[5] J. S. Allingham, A. Zampella, M. V. D'Auria, I. Rayment, *Proc. Natl. Acad. Sci. USA* **2005**, *102*, 14527–14532.
[6] V. A. Klenchin, J. S. Allingham, R. King, J. Tanaka, G. Marriott, I. Rayment, *Nat. Struct. Biol.* **2003**, *10*, 1058–1063.
[7] G. N. Murshudov, A. A. Vagin, E. J. Dodson, *Acta Crystallogr. Sect. D* **1997**, *53*, 240–255.
[8] P. J. McLaughlin, J. T. Gooch, H. G. Mannherz, A. G. Weeds, *Nature* **1993**, *364*, 685–692.

[9] V. A. Klenchin, R. King, J. Tanaka, G. Marriott, I. Rayment, *Chem. Biol.* **2005**, *12*, 287 – 291.
[10] E. J. Corey, K. C. Nicolaou, T. Toru, *J. Am. Chem. Soc.* **1975**, *97*, 2287 – 2288.
[11] S. A. Rizvi, V. Tereshko, A. A. Kossiakoff, S. A. Kozmin, *J. Am. Chem. Soc.* **2006**, *128* 3882 – 3883.
[12] J. D. Pardee, J. A. Spudich, *Methods Cell Biol.* **1982**, *24*, 271 – 289.
[13] T. Kouyama, K. Mihashi, *Eur. J.Biochem.* **1981**, *114*, 33 – 38.
[14] Z. Otwinowski, W. Minor, *Methods Enzymol.* **1997**, *276*, 307 – 326.
[15] P. Emsley, K. Cowtan, *Acta Crystallogr. Sect. D* **2004**, *60*, 2126 – 2132.
[16] CCP4, *Acta Crystallogr. Sect. D* **1994**, *50*, 760 – 763.

